A MASTER EQUATION THEORY OF FLUORESCENCE INDUCTION, PHOTOCHEMICAL YIELD, AND SINGLET-TRIPLET EXCITON QUENCHING IN PHOTOSYNTHETIC SYSTEMS

GUY PAILLOTIN
Service de Biophysique, Département de Biologie, Centre d'Etudes Nucléaires de Saclay, 91191 Gif sur Yvette, Cedex, France

NICHOLAS E. GEACINTOV
Chemistry Department, New York University, New York, New York 10003

JACQUES BRETON
Service de Biophysique, Département de Biologie, Centre d'Etudes Nucléaires de Saclay, 91191 Gif sur Yvette, Cedex, France

ABSTRACT A master equation theory is formulated to describe the dependence of the fluorescence yield (Φ) in photosynthetic systems on the number of photons (Y) absorbed per photosynthetic unit (or domain). This theory is applied to the calculation of the dependence of the fluorescence yield on Y in (*a*) fluorescence induction, and (*b*) singlet exciton-triplet excited-state quenching experiments. In both cases, the fluorescence yield depends on the number of previously absorbed photons per domain, and thus evolves in a nonlinear manner with increasing Y. In case *a*, excitons transform the photosynthetic reaction centers from a quenching state to a nonquenching state, or a lower efficiency of quenching state; subsequently, absorbed photons have a higher probability of decaying by radiative pathways and Φ increases as Y increases. In case *b*, ground-state carotenoid molecules are converted to long-lived triplet excited-state quenchers, and Φ decreases as Y increases. It is shown that both types of processes are formally described by the same theoretical equations that relate Φ to Y. The calculated $\Phi(Y)$ curves depend on two parameters m and R, where m is the number of reaction centers (or ground-state carotenoid molecules that can be converted to triplets), and R is the ratio $\Phi(Y \to \infty)/(Y \to 0)$. The finiteness of the photosynthetic units is thus taken into account. The $m = 1$ case corresponds to the "puddle" model, and $m \to \infty$ to the "lake," or matrix, model. It is shown that the experimental $\Phi(Y)$ curves for both fluorescence induction and singlet-triplet exciton quenching experiments are better described by the $m \to \infty$ cases than the $m = 1$ case.

INTRODUCTION

The instantaneous fluorescence and photochemical properties of photosynthetic systems often depend on the number of photons previously absorbed by the sample. One well-known example is the fluorescence induction phenomenon (1) in which the fluorescence yield increases with increasing illumination time; this effect is due to the transformation of the photochemically active reaction centers to the inactive state. Another example is the quenching of singlet excitons by carotenoid triplet excited states created by the previous absorption of photons (2–5). In both cases, the initial absorption of photons changes the subsequent fluorescence properties of the system. In the case of singlet-triplet quenching, the lifetime of the singlet excitons is decreased and the subsequent quantum yield of generation of additional triplet states is also reduced. The fluorescence yield is thus a complex function of the number of photons absorbed.

Simplified mathematical treatments of both fluorescence induction (1, 6, 7) and singlet-triplet quenching (2, 3, 5, 8) have been presented, but do not explicitly take into account the possible finite nature of the photosynthetic unit. The latter consists of a reaction center and the associated chlorophyll antenna molecules, or the number of carotenoid molecules per unit.

In this work a Master Equation Theory describing these phenomena is presented. The formulation of this theory is similar to the one presented earlier for singlet-singlet exciton annihilation (9). It is shown that the same equations for the instantaneous fluoresence yield ϕ, and the integrated (over the duration of an excitation pulse) fluo-

rescence yield Φ are formally valid for both the fluorescence induction and the singlet-triplet quenching cases. In this theory, it is assumed that the excitons are confined to domains consisting of a finite number of chlorophyll molecules, and in reaction centers (or carotenoid molecules). A parameter R, which denotes the relative fluorescence in the high and low limits of absorbed photons (Y), is defined. The fluorescence yields, fluorescence induction curves, and fraction q of transformed reaction centers (or carotenoid molecules in the triplet state), are calculated as a function of Y. These quantities depend on the parameters R and m, the size of the domains. As expected, the usual Poisson laws (10) apply for $m = 1$ (isolated photosynthetic unit), while for $m \rightarrow \infty$ the continuum equations (8) are applicable. However, these two extreme limits are also obtained for finite values of m and for certain values of R.

FORMULATION OF THE MODEL

Definition of Domains

We consider a system of N chlorophyll molecules that contains m ($m = 1, 2, 3, \ldots \infty$) possible quenching molecules and that is called a domain. Such domains are not necessarily characterized by any physical boundaries, but serve simply as a conceptual basis for the development of the model. This system has been previously utilized by us in formulating a Master Equation approach for treating singlet-singlet annihilations in photosynthetic membranes (9). As in the previous paper (9), we assume that the exciton motion from molecule to molecule is characterized by a hopping mechanism rather than by a coherent transfer mechanism, and we adopt the uniform or random approximation of exciton distributions. In this approximation it is assumed that the exciton spatial distribution is randomized within a time interval that is small compared with the characteristic bimolecular and unimolecular decay times of the singlet excitons. This approximation is discussed in more detail in the Appendix.

Types of Quenchers

Our model is applicable to three different types of quenching that are well-known in fluorescence studies of photosynthetic systems. Regardless of the type of quencher, these entities will be designated as Q in this work. The three types of quenching are:

(*a*) Quenching of singlet excitons by reaction centers of photosynthetic systems. It is well known that the fluorescence yield increases when the reaction centers (RC) are transformed from the "open" (quenching) state to the "closed" (nonquenching, or diminished quenching efficiency) state. This fluorescence increase is called fluorescence induction (1).

(*b*) The quenching of singlet excitons by triplet excited states. These quenchers are usually carotenoid triplets. As more and more photons are absorbed by a photosynthetic system, more triplets are created and the fluorescence yield decreases.

(*c*) Quenching of singlet excitons by extrinsic quenchers such as quinones or dinitrobenzene. Applications of this type of quenching have been described previously (2, 11).

The first two cases differ significantly from case *c*. In both *a* and *b*, the initial interaction of an exciton with the quencher (of which there are m per domain) transforms the latter from state Q_o to state Q_q. In case *a*, the exciton quenching efficiency of Q_o is greater than that of Q_q, while in case *b* the reverse is true. Therefore the fluorescence yield in both cases *a* and *b* depends on the number of quenchers transformed from Q_o to Q_q and thus on the number of photons previously absorbed. In case *c* the quenching of the fluorescence is independent of the number of photons absorbed.

In this work we are concerned with cases *a* and *b* only, and it is shown that both cases can be treated within the same framework and are formally quite similar.

The total rate of deactivation of singlet excitons is

$$K_i = k + k_{Q,i} \tag{1}$$

where

$$k = k_F + k_{IS} + k_D \tag{2}$$

is the unimolecular decay constant (k_F = radiative, k_{IS} = intersystem crossing, and k_D = nonradiative unimolecular decay constants), $k_{Q,i}$ is the bimolecular decay constant when a singlet exciton interacts with a quencher Q_q. The index i denotes the dependence of this rate constant on i, the number of quenchers in the state Q_q, according to

$$Q_o + \text{exciton} \rightarrow Q_q. \tag{3}$$

Thus, (i/m) is the fraction of quenchers in the state Q_q. We furthermore define the following rate constants,

$$k_{Q,o}\ (k_{Q,i} \text{ when } i = 0) \text{ and } k_{Q,m}\ (k_{Q,i} \text{ when } i = m). \tag{4}$$

In the case of the reaction centers (case *a*), $k_{Q,o} > k_{Q,m}$; in case *b*, $k_{Q,o}$ is assumed to be either zero, or $k_{Q,m} >> k_{Q,o}$ (quenching by triplets). In case *a*, m is the number of reaction centers per domain, in case *b* it is the number of carotenoid molecules that can ultimately be transformed to triplets.

When only i out of m quenchers are in the state Q_q, we can write

$$k_{Q,i} = (m - i)/m\, k_{Q,o} + (i/m)\, k_{Q,m} \tag{5}$$

and

$$K_i = k + (m - i)/m\, k_{Q,o} + (i/m)\, k_{Q,m} = (m - i)/m\, K_o + (i/m)\, K_m \tag{6}$$

where

$$K_o = k + k_{Q,o}, \text{ and } K_m = k + k_{Q,m}. \tag{7}$$

We also define the rate constant for the transformation of Q_o to Q_q (eq. 3), which is also a function of i:

$$K'_i = \frac{m - i}{m} \chi_o K_o \tag{8}$$

where χ_o is the quantum yield of formation of Q_q when $i = 0$. In general, when there are already i quenchers in a domain, the quantum yield of formation of the state Q_q is

$$\chi_i = \frac{K'_i}{K_i} = \chi_o \frac{(m - i)/m}{(m - i)/m + (i/m)(1/R)} \tag{9}$$

where

$$R = \frac{K_o}{K_m} \tag{10}$$

is an important parameter in the equations describing the dependence of the fluorescence on the number of absorbed photons, as is shown below; R defines the ratio of fluorescence yields for $i = m$ divided by the yield when $i = 0$; for case a, $R > 1.0$, while for case b $R < 1.0$.

FORMULATION OF THE MASTER EQUATION

The state of a domain is defined by two variables: i, $(0 \leq i \leq m)$, the number of quenchers that have already passed from the state Q_o to the state Q_q (Eq. 3), and n, the number of singlet excitons per domain.

The following transitions from one state of the domain to another state can be distinguished:

$(i, n) \rightarrow (i + 1, n - 1)$ rate constant K'_i (quenching of a singlet exciton accompanied by the transformation of an additional quencher from Q_o to Q_q)

$(i, n) \rightarrow (i, n - 1)$ rate constant $K_i - K'_i$ (quenching of an exciton without transformation of Q_o)

$(i, n) \rightarrow (i, n + 1)$ rate σI (creation of an exciton), σ is the absorption cross section per domain for the creation of an exciton, while I is the incident photon flux.

The rate constant $K_i - K'_i$ is the quenching rate constant of a singlet exciton that does not give rise to a $Q_0 \rightarrow Q_q$ transition. An important simplification in this scheme is that the lifetime of a Q_q state is much longer than the time scale of the experiment. This is a reasonable assumption in case b if the fluorescence measurements are performed with laser pulses that are less than ~ 1 μs in duration, since it is known that the lifetime of the carotenoid triplets is several microseconds long (2, 4, 5, 8). For case a this is also a reasonable assumption in most fluorescence induction experiments, since the Q_q state in chloroplasts is stable during the tens-of-seconds timescales of such experiments (12, 13).

We introduce the probability $p(i, n, t)$ that a given domain is in the state (i, n) at a time t. Its time dependence is

$$\begin{aligned}\frac{dp(i, n; t)}{dt} &= p(i, n + 1; t)(n + 1)(K_i - K'_i) \\ &+ p(i - 1, n + 1; t)(n + 1)K'_{i-1} - p(i, n; t)nK_i \\ &+ \sigma I\, p(i, n - 1); t) - \sigma I\, p(i, n; t).\end{aligned} \tag{11}$$

The origin of the different terms in Eq. 11 may be understood by referring to the diagram in Fig. 1. Each point on this two-dimensional diagram (maximum vertical dimension is m) denotes a possible state of the domain. Transitions other than the ones shown are neglected either on physical grounds, or within the context of the approximation that the i states do not decay on the time scale of the experiments that are described by this theory. The other assumptions are that the absorption of light throughout the sample is uniform and that the intensity I is sufficiently low that singlet-singlet exciton annihilations can be neglected.

Some generally valid relationships, without further approximations, can be deduced from Eq. 11 by introducing the following two quantities:

$$\langle n \rangle = \sum_{i,n} p(i, n; t) \text{ and } \langle i \rangle = \sum_{i,n} p(i, n; t)i \tag{12}$$

where $\langle n \rangle$ denotes the mean number of excitons per

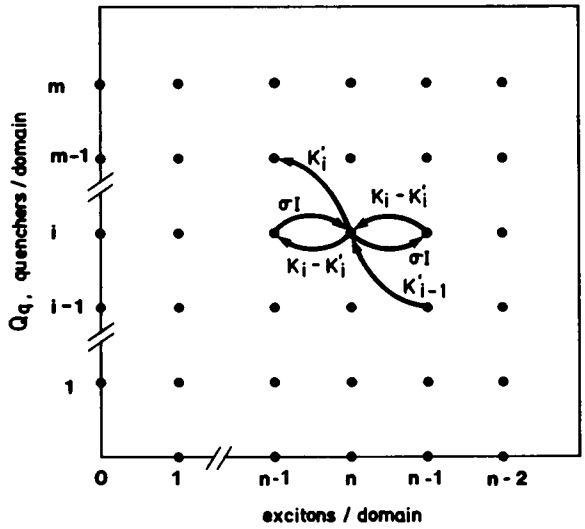

FIGURE 1 Two-dimensional representation of a domain and explanation of Eq. 11. There are a maximum number of m quenchers in the state Q_q (see Eq. 3); i is the actual number of quenchers in the Q_q state; n represents the number of excitons per domain. The various transitions to and from the state (n, i) and the relevant rate constants are depicted (see Eq. 11).

domain, while $\langle i \rangle$ denotes the mean number of quenchers in the state Q_q.

Utilizing Eq. 12, we obtain from Eq. 11

$$\frac{d\langle n \rangle}{dt} = \sigma I - K_o\langle n \rangle - (K_m - K_o)\left\langle n\frac{i}{m}\right\rangle \quad (13a)$$

$$\frac{d\langle i \rangle}{dt} = \chi_o K_o\langle n \rangle - \chi_o K_o\left\langle\frac{ni}{m}\right\rangle. \quad (13b)$$

These two coupled differential equations may be combined to yield the useful relationship

$$\frac{d\langle n \rangle}{dt} = \sigma I - K_m\langle n \rangle + \frac{K_m - K_o}{\chi_o K_o}\frac{d\langle i \rangle}{dt}. \quad (14)$$

Because of the discreteness of the domains, particularly when m is small, Eqs. 13 and 14 cannot be solved in the usual manner, and Eq. 11 must be used. On the other hand, Eqs. 13 and 14 can be simplified in the case of very large domains ($m \rightarrow \infty$, the continuum case) by setting $\langle ni/m \rangle \sim \langle n \rangle \langle i/m \rangle$; furthermore, as will be shown below, these equations are also useful in the steady-state case, $d\langle n \rangle / dt = 0$, or, integrated over an entire excitation pulse, $\int_0^\tau d\langle n \rangle/dt = 0$, where τ is the duration of a pulse.

The solution of Eq. 11 is possible under certain restrictive, though physically realistic conditions. We first define the quantities

$$p_i(t) = \sum_n p(i, n; t), \qquad n_i(t) = \sum_n p(i, n; t)n \quad (15)$$

where p_i is the probability that there are i quenchers in a domain, while n_i is the mean number of excitons when there are i quenchers in a domain. Under conditions of excitation intensities such that

$$\sigma I \text{ and } \frac{dI}{Idt} \ll K_o, K_m, \quad (16a)$$

the condition

$$n_i(t) \lesssim 1 \quad (16b)$$

should prevail. To ensure that the number of excitons per domain is unity or less, their rate of creation by light absorption must be $< K_o \approx 10^9\ s^{-1}$, since the lifetime of singlet excitons in photosynthetic systems is of the order of ~1 ns (1). Furthermore, the intensity I should not exhibit strong variations on the nanosecond time scale, either. It is shown in the Appendix that, when these conditions are fulfilled

$$n_i(t) = \frac{\sigma I}{K_i}p_i(t) \quad (17)$$

$$\frac{dp_i(t)}{\sigma I\, dt} = -\chi_i p_i(t) + \chi_{i-1}p_{i-1}(t). \quad (18)$$

It should be noted that Eq. 11 can also be solved exactly for the case of a delta-pulse excitation (for example, picosecond laser-pulse excitation), by setting the σI terms in Eq. 11 equal to zero. Only the case of nanosecond duration pulse excitation (fluctuations in I on the time-scales of K_o^{-1}) is difficult to solve exactly.

CALCULATION OF EXPERIMENTALLY OBSERVABLE QUANTITIES

The experimentally measurable quantities are the following: f, the instantaneous fluorescence intensity; ϕ, the instantaneous fluorescence yield; Φ, the integrated fluorescence yield resulting from an excitation pulse, and $q = \langle i/m \rangle$, the fraction of quenchers in the Q_q state.

In Eq. 18, $p_i(t)$ depends upon the time. Because q, and therefore ϕ and Φ, depend upon the history of the domain (i.e., the number of total photons previously absorbed), it is useful to express $p_i(t)$ as $p_i(Y_t)$, where Y_t is the number of photons absorbed between the onset of the excitation at $t = 0$, and the time t:

$$Y_t = \int_0^t \sigma I(t')\, dt'. \quad (19)$$

If $I(t')$ is constant, then $Y_t = \sigma I t$. If pulse-excitation is utilized, and if the duration of the pulse is $t = \tau$, then the total number of photons absorbed per pulse is

$$Y = \int_0^\tau \sigma I(t')\, dt'. \quad (20)$$

Eq. 18 may be rewritten in terms of the variable Y_t:

$$\frac{dp_i(Y_t)}{dY_t} = -\chi_i p_i(Y_t) + \chi_{i-1}p_{i-1}(Y_t) \quad (21)$$

where p_i is now a function of Y_t. The experimentally observable variables may now be further defined:

(*i*) f, the instantaneous fluorescence intensity at time t, after Y_t photons had been absorbed:

$$f = k_F \sum_i n_i(Y_t) = \sigma I \sum_i p_i(Y_t)\phi_i \quad (22)$$

where $\phi_i = (k_F/K_i)$ is just the instantaneous fluorescence yield when there are i quenchers in a domain. The overall instantaneous fluorescence yield $\phi\,(Y_t)$ is

$$\phi(Y_t) = \frac{f}{\sigma I} = \sum_i p_i(Y_t)\phi_i. \quad (23)$$

(*ii*) The total fluorescence F emitted during the course of an excitation pulse of duration τ

$$F = k_F \sum_i \int_0^\tau n_i(t)\, dt = \int_0^Y \phi(Y_t)\, dY_t \quad (24)$$

and the integrated fluorescence yield Φ, defined as

$$\Phi = (F/Y) = 1/Y \int_0^Y \phi(Y_t)\, dY_t. \quad (25)$$

(*iii*) While ϕ and Φ are the instantaneous and integrated fluorescence yields that are observed experimentally, it is

useful to define the analogous normalized quantities ϕ' (Y_t) and Φ' (Y_t), which range in value between 0 and 1:

$$\phi'(Y_t) = \frac{\phi(Y_t) - \phi_m}{\phi_0 - \phi_m} = \sum_i p_i(Y_t)\phi_i' \tag{26}$$

$$\phi_i' = \frac{\phi_i - \phi_m}{\phi_0 - \phi_m}. \tag{27}$$

ϕ_i is the instantaneous fluorescence yield when there are i quenchers in a domain, ϕ_0 and ϕ_m are the corresponding quantities when $i = 0$ $(Y_t = 0)$ and when $i = m$ $(Y_t \rightarrow \infty)$, when all quenchers have passed into the state Q_q.

In view of Eq. 10, the parameter R can also be expressed as

$$R = \frac{K_0}{K_m} = \frac{\phi_m}{\phi_0}. \tag{28}$$

Similarly, we define the normalized integrated fluorescence yield

$$\Phi' = \frac{\Phi - \phi_m}{\phi_0 - \phi_m} = \frac{1}{Y}\int_0^Y \phi'(Y_t)\, dY_t. \tag{29}$$

The relationships between the experimentally measurable quantities ϕ (Y_t) and Φ (Y), the limiting values ϕ_0 and ϕ_m, and the normalized, calculable quantities ϕ' (Y_t) and Φ' (Y) are depicted in Fig. 2. Two examples are given corresponding to $R = \phi_m/\phi_0 = 4$ and $R = 0.1$. The first is an example of the general case *a* in which $R > 1.0$ and fluorescence induction occurs, and the other one corresponds to case *b*, $R < 1.0$, fluorescence quenching by photoinduced triplets.

(*iv*) Determination of the fraction $q = \langle i/m \rangle$, the mean number of quenchers in the Q_q state. This quantity can be evaluated from Eq. 14. For any excitation of duration τ in which Y photons have been absorbed, we obtain

$$\int_0^\tau \frac{d\langle n \rangle}{dt}\, dt = 0, \int_0^\tau \langle n \rangle\, dt = \frac{F}{k_F} = \frac{Y}{k_F}\Phi.$$

Integrating Eq. 14 we obtain

$$q = \left\langle \frac{i}{m} \right\rangle = \sum_i p_i(Y_t)(i/m) = q_0 + \frac{\chi_0}{m}\int_0^Y \phi'(Y_t)\, dY_t = q_0 + \frac{\chi_0}{m} Y\Phi' \tag{30}$$

where q_0 is the value of q at the onset of the pulse at $t = 0$ $(Y_t = 0)$. It should be noted that Eq. 30 is quite general since it has been obtained from Eq. 14 without the special limiting conditions defined in Eq. 16. The fraction of quenchers in the Q_q state is proportional to Y/m, the number of photons absorbed per quencher; χ_0, the intrinsic quantum yield of formation of the Q_q state; and Φ', the normalized integrated fluorescence quantum yield. Thus, q can be obtained from experimentally determined values of ϕ (Y_t) and Φ (Y), from which ϕ' (Y_t) and Φ' (Y) can be obtained. In experiments of fluorescence induction, the

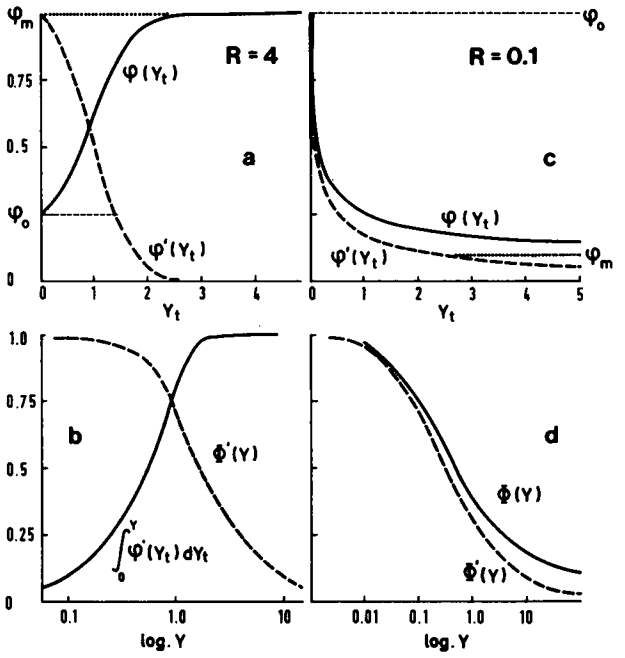

FIGURE 2 Explanation of measurable (———) and calculated (·····) quantities; ϕ (Y_t) and ϕ' (Y_t) are the measured and normalised instantaneous fluorescence yields when Y_t photons have already been absorbed by the sample at time t. Φ (Y) and Φ' (Y) are the fluorescence yields integrated over an entire excitation pulse (duration τ, total photons absorbed Y). The solid line in *b* is the "work-integral"—see text. *a* and *b* show fluorescence induction, *c* and *d* show fluorescence quenching. While the solid lines are meant to represent actual experimental observables, the curves shown have been calculated utilizing Eqs. 45 and 48 $(m \rightarrow \infty)$ and the Definitions 26 and 29, utilizing the R values given in the figure. For case *a*, R > 1.0; for case *b*, $R < 1.0$.

quantity $\int_0^Y \Phi'$ (Y_t) dY_t in Eq. 30 is known as the "work integral" (1). It can be directly obtained from such experiments, and its dependence on Y is also shown in Fig. 2.

EXPLICIT CALCULATIONS OF ϕ' (Y_t) and Φ' (Y)

It is evident from the previous section that, to compare experimental results with those of the theory, explicit values of ϕ' (Y_t) and Φ' (Y) must be calculated. For the general case of finite m, the starting point for such calculations is Eq. 21; the parameters of the theory are the number of photons absorbed (Y_t or Y), the relative fluorescence yield parameter R (Eq. 28) and m, the dimension of the domain. When $m \rightarrow \infty$, the continuum case (Eq. 13) can be solved directly.

The explicit derivations are given in the Appendix. We obtain:

$$\phi'(Y_t) = \sum_{i=0}^{m-1} p_i(0) \left\{ \sum_{j=1}^{m-1} \cdot C_{m-i}^{j-1} \frac{R(1-R)^{m-1-j}}{m^{m-i-1}} (m-j)^{m-j} \times [j + (m-j)R]^{j-i-1} e^{-\chi_j Y_t} \right\} \tag{31}$$

and

$$\Phi'(Y) = \int_0^Y \phi'(Y_t)\,dY_t = \frac{1}{\chi_0 Y}\sum_{i=0}^{m-1} p_i(0) \cdot \left\{(m-i) - \sum_{j=1}^{m-1} C_{m-i}^{j-1}\frac{(1-R)^{m-1-j}}{m^{m-i-1}}(m-j)^{m-j-1} \times [j+(m-j)R]^{j-i}\, e^{-\chi_j Y}\right\}. \quad (32)$$

The factor C_{m-i}^{j-1} is defined, as usual, by

$$C_{m-i}^{j-1} = \frac{(m-i)!}{(j-i)!(m-j)!}. \quad (33)$$

The quantity p_i (o) is the probability that at $t = 0$ ($Y_t = 0$) there are already i quenchers present in a domain. In our discussion in this work, we assume that none of the quenchers Q_o have been previously transformed to the state Q_q. Thus all terms p_i (o) = 0 ($i \geq 1$) and p_o (0) = 1.0. Thus the double sums in Eqs. 31 and 32 reduce to single sums. It should be noted that when, in general, $p_i \neq 0$ (for $i \neq 0$), and if the quenchers are initially distributed at random, then

$$p_i(o) = C_m^i\, q_o^i\,(1-q_o)^{m-i} \quad (34)$$

where q_o is the average initial concentration, and Eq. 34 is just the binomial distribution.

Using p_o (o) = 1, p_i (o) = 0 ($i \neq 0$), some of the equations for $\phi'(Y_t)$ and $\Phi'(Y)$ for the first few possible values of m are given below:

(*a*) $m = 1$

$$\phi'_{(1)}(Y_t) = e^{-\chi_0 Y_t} \quad (35)$$

$$\Phi'_{(1)}(Y) = \frac{1}{\chi_0 Y}(1 - e^{-\chi_0 Y}). \quad (36)$$

It is evident that these equations are also obtained from Eqs. 31 and 32 for any finite value of m when $R = 0$ ($Rm = 0$) since $\chi_i = 0$ (for any value of $i \neq 0$, according to Eq. 9). Eq. 36 follows directly from a consideration of a Poisson distribution of photon hits per domain; this equation has been previously obtained by Mauzerall (14).

(*b*) $m = 2$

$$\phi'_{(2)}(Y_t) = (1-R)e^{-\chi_0 Y_t} + Re^{-\chi_1 Y_t} \quad (37)$$

$$\Phi'_{(2)}(Y) = \frac{1}{\chi_0 Y}[2 - (1-R)e^{-\chi_0 Y} - (1+R)e^{-\chi_1 Y}] \quad (38)$$

(*c*) $m = 3$

$$\phi'_{(3)}(Y_t) = (1-R^2)e^{-\chi_0 Y_t} + (4/3)R(1-R)e^{-\chi_1 Y_t} + \frac{R(2+R)}{3}e^{-\chi_2 Y_t} \quad (39)$$

$$\Phi'_{(3)}(Y) = \frac{1}{\chi_0 Y}\left[3 - (1-R)^2 e^{-\chi_0 Y} - (2/3)(1-R) \cdot (1+2R)e^{-\chi_1 Y} - \frac{(2+R)^2}{3}e^{-\chi_2 Y}\right]. \quad (40)$$

Another important case is the continuum case, for which m is very large. We now consider this case in some detail:

(*d*) $m \to \infty$.

When $m \to \infty$, Eq. 13 can be further simplified since, in large domains $\langle ni/m\rangle = \langle n\rangle q$. We thus obtain

$$\frac{d\langle n\rangle}{dt} = \sigma I - K_o\langle n\rangle - (K_m - K_o)\langle n\rangle q \quad (41a)$$

$$\frac{dq}{dt} = \frac{\chi_o K_o}{m}\langle n\rangle (1-q). \quad (41b)$$

We solve these equations for the case of pulse excitation which gives $\int_0^\tau d\langle n\rangle = 0$. By first integrating Eq. 41b we obtain the quantity $-\ln(1-q)$ which, upon appropriate substitution in Eq. 41a, gives

$$RX = -(1-R)q - \ln(1-q) \quad (42)$$

where we have expressed the number of absorbed photons per quencher which transforms this quencher from the Q_o to the Q_q state by

$$X = \frac{\chi_o Y}{m}. \quad (43)$$

By making the appropriate substitutions $mX = \chi_o Y$ in Eqs. 35–40, it is convenient to evaluate these latter equations in terms of X rather than of $\chi_o Y$.

Using the relation obtained from Eq. 30 with $q_o = 0$ we obtain

$$q = X\Phi' \quad (44)$$

and

$$RX = -(1-R)X\Phi' - \ln(1 - X\Phi'). \quad (45)$$

Using this equation, Φ' as a function of X can be easily evaluated by assuming appropriate values of $X\Phi'$ and substituting these in Eq. 45, thus solving for X, and then using Eq. 44 to solve for the corresponding value of Φ'.

When $R \to 0$, it is evident that $X\Phi' \approx 0$ is a valid solution of Eq. 45. Under these conditions, the logarithmic term in Eq. 45 can be expanded, and we obtain

$$\Phi' \approx \frac{(1+2X/R)^{1/2} - 1}{X/R} \quad (\text{for } R \to 0). \quad (46)$$

If R $\approx$ 1.0, Eq. 45 reduces to Eq. 36, i.e., the Poisson law. It can be shown that Φ' does not significantly deviate from Poisson-like behavior as long as R is near unity.

SOME CALCULATED EXAMPLES OF Φ' (Y)

Utilizing Eq. 45 ($m \to \infty$), we have calculated the dependence of Φ' as a function of X for different values of the fluorescence quenching parameter R. While the experi-

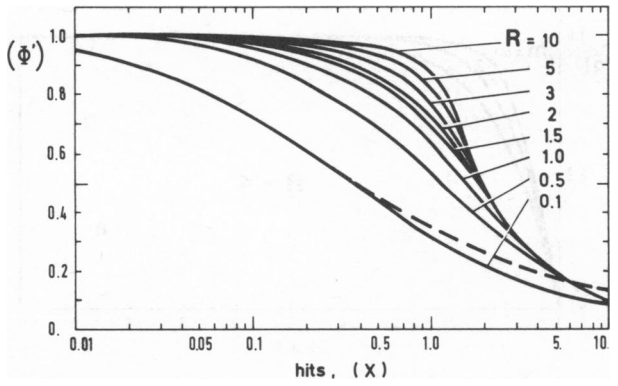

FIGURE 3 Calculations of integrated normalized fluorescence yields Φ' for different values of R for $m \rightarrow \infty$, using Eq. 45. X is the number of effective photon hits per quencher (transforming the latter from $Q_o \rightarrow Q_q$. The dashed line was obtained with Eq. 46, showing that Eqs. 45 and 46 do not give the same results for $R = 0.1$.

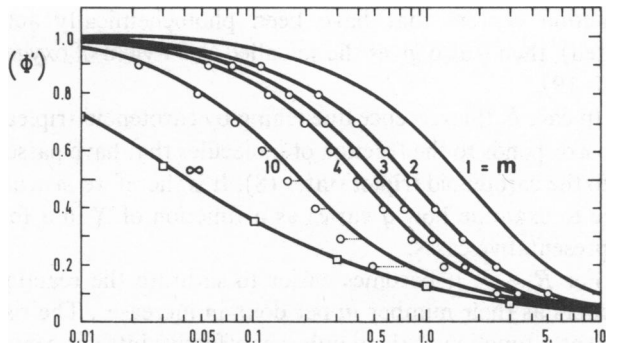

FIGURE 4 Calculations of Φ' as a function of X for $R = 0.01$ for different values of m. For $m < 10$ the curves have been calculated utilizing Eq. 32. The $m = \infty$ (solid line) is calculated utilizing Eq. 45; □, points calculated from Eq. 46, showing that these two equations give the same results for $R = 0.01$. ○, values calculated from the pseudo-Poisson case, Eq. 47, by displacing the $m = 1$ curve along the horizontal axis by an amount $\sim X/m$.

mentally measured fluorescence yields Φ increase with increasing X for $R > 1.0$, and Φ decreases for $R < 1$, the corresponding Φ' values decrease in both types of cases (see Fig. 2).

For $R = 1$, the dependence is given by the Poisson law (Eq. 36). The dependence of Φ' on X for $m = \infty$ and for different values of R is shown in Fig. 3. These curves have been calculated according to Eq. 45. Similar calculations of Φ' for different values of m, but for the same value of $R(= 0.01)$ are shown in Fig. 4. The $m = 1$ case, of course, is the Poisson case. It is interesting to note that the shapes of the curves for $R < 4$ in the examples shown deviate only to a negligible extent from that of the pure Poisson case ($m = 1$). However, for increasing m, the curves are displaced to the left along the horizontal axis by intervals corresponding to $[X(m = 1)]/m = X\,(1 < m \lesssim 6)$. Thus we can write

$$\Phi'(X) \approx \frac{1}{mX}(1 - e^{-mX}) \quad \text{for } R < 0.01,\ 1 \leq m \lesssim 6 \quad (47)$$

and the Poisson-like behavior is observed for approximately $m \lesssim 6$. The smaller the value of R, the larger the value of m for which Eq. 47 is still applicable. For a given value of R, the deviation of Φ' from Poisson-like behavior is larger, the larger the value of m. In such cases, exact Eq. 32, using Relationship 43, must be utilized to evaluate $\Phi'(X)$ for finite m. When $m = \infty$, Eq. 45 should be used.

In Fig. 4 it is evident that the approximation Eq. 46 is a good one for $R = 0.01$ but deviates significantly from Eq. 45 for $r = 0.1$. Thus, Eq. 46 can be used only in the case of very strong quenching (small R).

To summarize this section, the appropriate equations (32, 36, 45, 46 or 47) to be used depend on the values of R and m. The appropriate conditions under which each of these equations is applicable is summarized in Table I.

SOME CALCULATIONS OF q, THE FRACTION OF QUENCHERS IN THE Q_q STATE

We consider the situation in which the initial concentration of quenchers in the domain is zero ($q_o = 0$ in Eq. 30). The fraction $q = \langle i/m \rangle$ can be easily evaluated using calculated values of Φ' in conjunction with Eq. 44. The parameter q in case a, fluorescence induction, corresponds to the fraction of reaction centers that have been closed. This quantity can be measured experimentally (6, 15, 16). In addition, if we assume that the photochemical yield (e.g., oxygen evolution), even though it consists of multiple photo-induced steps, is proportional to q (the fraction of

TABLE I
CALCULATION OF FLUORESCENCE YIELDS FOR DIFFERENT RANGES OF THE PARAMETERS m AND R

m	$R = 0$	$R \lesssim 0.01$	$R = 1.0$ (or ≈ 1.0)	$R \approx$ finite ($\neq 0, \neq 1$)
$m = 1$	Poisson	Poisson	Poisson	Poisson
$m = 2 \sim 6$	Poisson	pseudo-Poisson	Poisson	general case
$6 \lesssim m \ll \infty$	Poisson	general case	Poisson	general case
$m \rightarrow \infty$	Poisson	continuum	Poisson	continuum

Evaluation of the normalized fluorescence quantum yield $\Phi'(X)$ as a function of the number of effective photon hits per quencher. Directory of equations to be used for different values of m (quenchers per domain), and R (the ratio of high intensity/low intensity fluorescence yield).
The equations can be found in text as noted: Poisson, Eq. 36; pseudo-Poisson, Eq. 47; general case, Eq. 32 (with $mX = \chi_o Y$); continuum, Eq. 45, for last column, and Eq. 46 for $R \lesssim 0.01$ column, an approximation of Eq. 45.

reaction centers that have been photochemically activated), then q also gives the so-called flash-yield of oxygen (17–19).

In case *b*, fluorescence quenching by carotenoid triplets, q corresponds to the fraction of molecules that have passed into the carotenoid triplet states (8). It is therefore instructive to examine how q varies as a function of X in a few representative cases.

For $R = 4$, it becomes easier to saturate the reaction centers as their number m per domain increases. The rise of q as a function of the number of effective hits per center is exponential for $m = 1$. An exponential Poisson dependence has been recently observed for the oxygen yield in *Chlorella* as a function of photon hits by Ley and Mauzerall (19). In other experiments, however, nonexponential behavior is often observed for the photochemical yield in photosynthetic systems (17, 20). There is little difference between the $m = 1$ and the $m = 2$ curves. These differences diminish as R becomes smaller than 4 and approaches unity. Thus, the type of curves depicted in Fig. 5 *a* tend to merge for small values of R near unity and for small values of m. It is thus possible to observe an exponential rise of q even for $m = 2, 3, 4 \ldots$, as long as the value of R is smaller than 4. The exponentiality is better the closer R is to unity.

The behavior of $q(X)$ is quite different when Q_q is a stronger fluorescence quencher than Q_o (case *b*). Some typical curves calculated for $m = 1, 2, 3$ and ∞ are shown in Fig. 5 *b*. For the $m = 1$ case, q displays exponential behavior as in Fig. 5 *a*. For the $m = 2$ case, q tends to approach saturation when $q = \langle i/m \rangle \approx 0.5$; for the $m = 3$ case this occurs when $q \approx 0.33$. This follows from the $R = 0.01$ condition, which implies that Q_q is a very strong fluorescence quencher, relative to the quenching ability of Q_o. Thus, the first hit per domain produces the transformation of one of the quenchers from Q_o to Q_q, thus producing one quencher per domain. Subsequent hits are much less effective in producing additional Q_q states because of the strong quenching ability of the first Q_q. Therefore, in general, there is a sharp levelling off in the $q(X)$ curves when $q = \langle i/m \rangle \approx 1/m$, i.e., when there is one quencher per domain.

In the continuum case (for $m = \infty$), there is a sharper initial rise, and a slower rise in q as X increases. Similar behavior has been experimentally observed by Breton et al. (8) for the quenching of the fluorescence in chloroplasts by carotenoid triplet states.

SOME CALCULATIONS OF INSTANTANEOUS FLUORESCENCE YIELDS, ϕ (Y_i)

In the steady-state approximation (Eq 16) and for $m = \infty$, Eq. 41 can be solved for ϕ ($= \langle n \rangle / \sigma I$), giving

$$\frac{\phi}{\phi_m} = \frac{1}{R + (1 - R)q}. \tag{48}$$

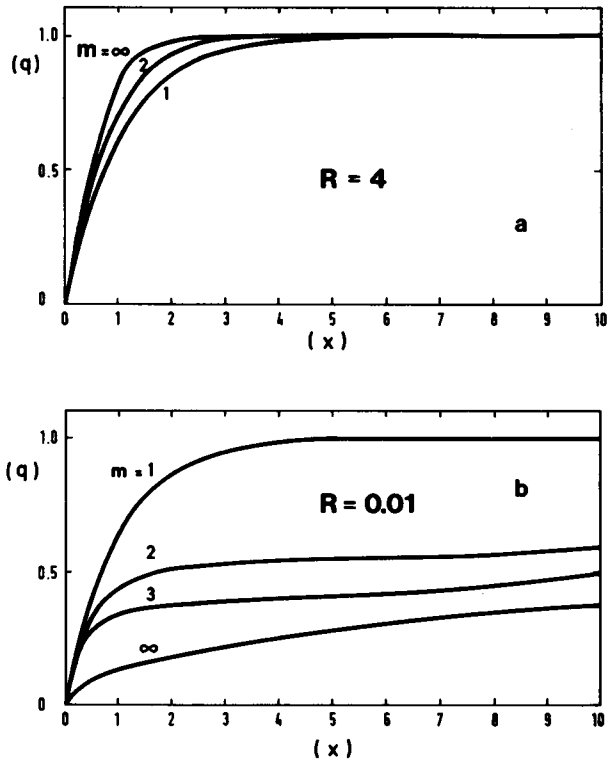

FIGURE 5 Calculations of $q = \langle i/m \rangle$ as a function of effective photon hits X, the fraction of quenchers transformed to the Q_q state. In case *a*, this would correspond to the fraction of oxidized (closed) reaction centers. In case *b*, q is the fraction of carotenoid molecules in the triplet state.

This is a form of the familiar Stern-Volmer equation. If excitation pulses are utilized, ϕ can also be obtained from

$$\phi = \frac{d}{dx}(X\Phi). \tag{49}$$

Values of q for different values of X can be calculated as outlined in the previous section, and then the relative instantaneous fluorescence yield can be evaluated from Eq. 48 for $m = \infty$. In fluorescence induction experiments, the instantaneous fluorescene yield increases from a value of ϕ_o to a value of ϕ_m as q varies between 0 and 1. By making the assumption that $X \propto$ time Eq. 48 can be used to calculate induction curves. Several such curves are illustrated in Fig. 6. An exponential induction curve for $m = 1$ is shown for reference. For $R = 4$, which is a typical value in fluorescence induction experiments with chloroplasts the induction curve shows the typical sigmoid behavior (for $m = \infty$). However, as the value of R decreases, the sigmoidal behavior becomes less prominent and practically disappears for $R \leq 2$. This is an important point to note, since in practice it is frequently observed that fluorescence induction curves that are initially sigmoidal can become exponential depending on preillumination conditions (13, 21) or the redox potential (22). The behavior depicted in Fig. 6 shows that even in so-called "multi-central" units, or the continuum or lake model, the induction curves display

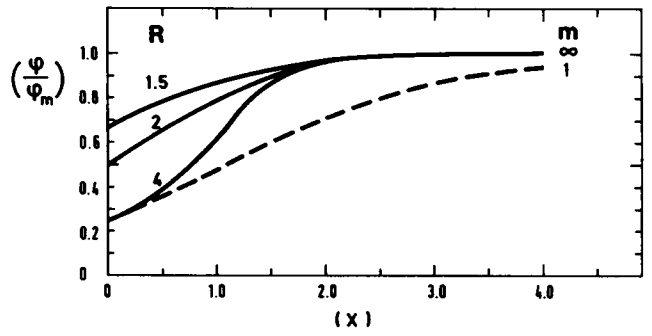

FIGURE 6 The dependence of the shapes of fluorescence induction curves on the parameter $R = \phi_m/\phi_o$, where ϕ_o is the initial and ϕ_m (normalized to unity) is the final fluorescence yield. The parameter X (Eq. 43) is proportional to the number of photons absorbed. These induction curves can be compared with those measured experimentally in which the time, rather than the intensity, of the illumination is varied (1, 12 13), by noting that $X \propto$ time in such experiments (assuming constant light intensity after the onset of illumination). The data for R = 1.5, 2, and 4 have been calculated for the $m = \infty$ (lake model) case, while the exponential $m = 1$ case (which is independent of R!) is appropriate for the puddle model (-----).

exponential behavior when R is small. Thus, the ratio of the final to the initial fluorescence yields must be carefully considered before conclusions based on sigmoidicity of fluorescence induction curves can be reached.

Another interesting quantity to examine is the dependence of ϕ_m/ϕ on q for different values of m and for R = 0.01 (Fig. 7). In these calculations, ϕ' (Y_t) was first evaluated from Eq. 31 using $mX = \chi_o Y_t$, ϕ was then calculated from Eq. 26. The quantity q was determined from Eq. 30 (with $q_o = 0$) after obtaining Φ' from Eq. 32. It is evident from Fig. 7 that an abrupt rise in ϕ_m/ϕ occurs when $q \approx 1/m$. The reasons for this behavior are evident from Fig. 5 and the associated discussion. At these particular values of q, corresponding to one quencher per domain, there is a drastic decrease in ϕ as q increases from 0 to $\sim 1/m$; for $q > 1/m$ the change in the fluorescence yield is less severe. This may also be seen qualitatively in Fig. 2 (see also Fig. 3 of reference 8); there is a relatively sharp drop in ϕ (Y_t) when Y_t is small (cf. Fig. 5), followed by a much smaller rate of decrease as Y_t increases further. As m becomes larger and larger, the ϕ_m/ϕ vs. q. plot approaches a straight line as predicted by Eq. 48 for the continuum case; for $R = 0.01$, the slope of such a straight line is 0.99, and its $q = 0$ intercept is 0.01.

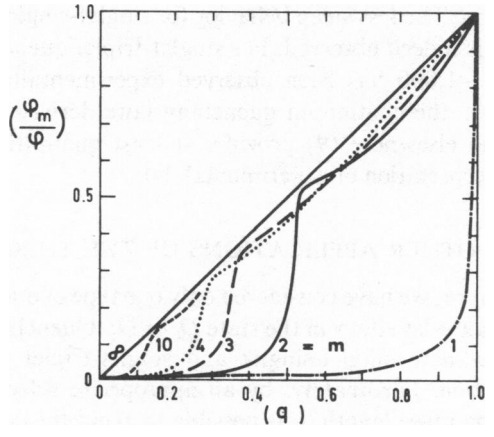

FIGURE 7 Stern-Volmer-type plots of reciprocal instantaneous fluorescence yields ϕ as a function of q (fraction of triplet excited carotenoids) for different values of m, for R = 0.01.

The results shown in Fig. 7 demonstrate that appropriate parallel determinations of ϕ_m/ϕ and of q could give important information on the value of m, i.e., the dimensionality or size of the domain. This behavior can, in principle, be tested by monitoring the intensity (and thus q) dependence of the fluorescence yield of chlorophyll-protein complexes and their agreggates, which constitute domains of varying sizes. It should be pointed out, however, that it may be difficult experimentally to achieve values of $q \gg 1/m$ (see Fig. 5).

In fluorescence induction experiments it is customary to plot $(\phi_m/\phi) - 1$ vs. $1 - q$, the fraction of open reaction centers (Stern-Volmer plots). Because the fluorescence quenching efficiency of the open centers (Q_o) is higher than that of the closed reaction centers (Q_q), the Stern-Volmer equation should give, in the continuum case, a straight line with positive slope when ϕ_m/ϕ is plotted as a function of $1 - q$, the fraction of centers in the Q_o state. Rearranging Eq. 48, we obtain

$$\frac{\phi_m}{\phi} - 1 = (R - 1)(1 - q). \tag{50}$$

Such a straight line plot for $R = 4$ is compared in Fig. 8

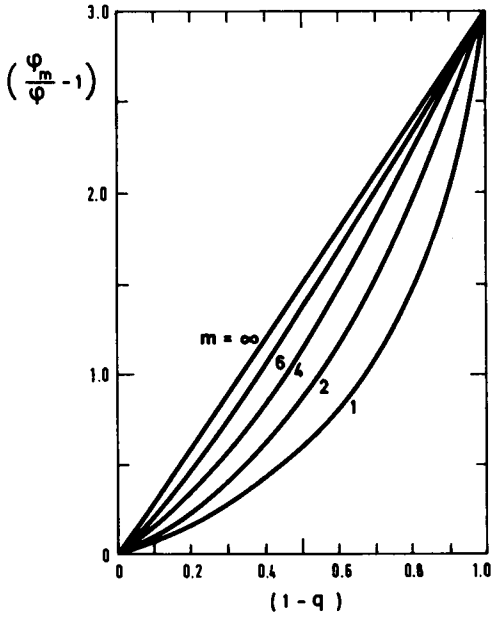

FIGURE 8 Stern-Volmer-type plots of reciprocal fluorescence yields for the fraction of reaction centers in the Q_o (open) state for R = 4 (fluorescence induction case) as a function of $1 - q$.

with similar plots calculated from Eq. 31 for different values of m. The Stern-Volmer law appears to be a good approximation for ϕ as long as $m > 6$. Fluorescence induction measurements can thus also provide information on the size of the photosynthetic domains. Both Clayton (16) and more recently van Gorkom et al. (15) have reported for photosynthetic bacteria and for chloroplasts, respectively, that Stern-Volmer type plots are obtained when ϕ_m/ϕ is plotted as a function of $1 - q$. These results indicate that there are many reaction centers per domain in these systems, i.e., that the domains are large. However, it should be kept in mind that the existence of more than one quenching state of reaction centers (23) and a heterogeneity of photosystems have been proposed. These additional complexities, while they can be easily introduced into our model, have not been taken into account here.

CONNECTION BETWEEN THIS THEORY AND BRETON ET AL.'S LAKE MODEL (8) OF SINGLET-TRIPLET EXCITON QUENCHING

Breton et al. studied the time dependence of the fluorescence yield (8) and the integrated fluorescence yield (24) as a function of laser pulse intensity. A microsecond duration pulse was used so that the conditions (16) were satisfied and the quenching of the fluorescence was attributed to carotenoid triplet excited states. A continuum model was adequate (8) for accounting for the dependence of q (the concentration of carotenoid triplets) on the laser intensity, and of ϕ (Y_t). In their model, the concentration of triplets was denoted by n_T and that of the singlets by n_S. A bimolecular singlet-triplet exciton quenching constant γ_{ST} was defined whose value was found to be $10^{-8}\text{cm}^3\text{s}^{-1}$. The value of γ_{ST} is similar to the value of $\gamma_{SS} = 5.10^{-9}\text{cm}^3\text{s}^{-1}$ found for singlet-singlet exciton quenching (25).

If we define the volume of a domain by V, then the following relations connect the variables used in this work to those of Breton et al.

$$n_S = \frac{\langle n \rangle}{V},$$

$$n_T = (car_T) = \langle i \rangle / V, \quad (car_o) = m/V, \quad \alpha = \sigma/V. \quad (51)$$

Here (car_o) denotes the same thing as Q_o, the number of ground-state carotenoid molecules that can be converted to triplets (car_T).

With these definitions, Eq. 41a reduces to

$$\frac{dn_S}{dt} = \alpha I - k\, n_S - \frac{k_{Q,m}}{(car_o)} n_S n_T = \alpha I - k n_S - \gamma_{ST} n_S n_T \quad (52)$$

where $\gamma_{ST} = (k_{Q,m})/(car_o)$. This equation is the same as the one used by Breton et al. (8).

COMPARISON BETWEEN SINGLET-SINGLET AND SINGLET-TRIPLET EXCITON QUENCHING CURVES

These quenching curves are defined as plots of the integrated fluorescence yield Φ (or Φ') as a function of the relative number of photons incident on the sample (or absorbed by the sample). We shall confine ourselves to the continuum quenching laws, since the $m \to \infty$ case has been found to be appropriate for describing singlet-singlet exciton annihilation quenching curves (9, 25) according to the equation, first derived by Swenberg et al. (26)

$$\Phi_{SS} = (1/X) \log (1 + X). \quad (52)$$

(The parameter X in this equation, since it pertains to singlet annihilation, is different from the one defined in this work. However, X is in all cases a linear function of the number of photons absorbed; thus the ratios of intensities that are important in this discussion are independent of the differences in proportionality constants.)

We shall calculate the intensity ratios

$$\frac{X_{0.1}}{X_{0.9}} \quad (53)$$

where $X_{0.1}$ and $X_{0.9}$ are the relative intensities corresponding to $\Phi' = 0.10$ and 0.90, respectively. Therefore, the ratio (Eq. 53) is a measure of the "steepness" of the fluorescence quenching curves, or of how rapidly Φ' decreases with increasing X. We find the following:

Poisson quenching law (Eq. 36)	$X_{0.1}/X_{0.9} \approx 50$
Singlet-singlet quenching (Eq. 52)	$X_{0.1}/X_{0.9} \approx 150$
Singlet-triplet quenching (Eq. 46)	$X_{0.1}/X_{0.9} \approx 730.$

Thus, the steepest decrease (smallest ratio) in Φ is expected for a pure Poisson quenching law, which has not been observed either for singlet-singlet, or singlet-triplet quenching. The less steep behavior for singlet-singlet annihilation is indeed observed. For singlet-triplet quenching a ratio of ~1,000 has been observed experimentally (24). Therefore, the continuum quenching laws derived in this work and elsewhere (9) provide, at least qualitatively, a good interpretation of experimental data.

OTHER APPLICATIONS OF THE THEORY

In this work, we have considered only one type of quencher, which can exist either in the state Q_o or Q_q. Quenching can occur by both singlet-singlet and singlet-triplet exciton annihilation. Fortunately, by an appropriate selection of excitation pulse length, it is possible to avoid the competition between singlet-singlet and singlet-triplet exciton annihilation (24). Other types of competition between

different types of quenchers can be easily treated by generalizing the theory derived here. Some examples are:

(*i*) Two or more types of reaction centers (23) or photosynthetic units (18, 22). Exact treatment of fluorescence induction curves is possible.

(*ii*) Competition between quenching of excitons by carotenoid triplet states and by open reaction centers. A detailed study of such effects, including an experimental determination of the fraction of reaction centers that remain open, and the number of excited carotenoid triplets produced, could give information on the relative locations of these species in photosynthetic systems.

(*iii*) Competition between singlet-singlet exciton annihilation and exciton capture by open reaction centers. A detailed consideration of these effects by this theory may provide new information on the rate of exciton caputre by reaction centers since the bimolecular exciton annihilation coefficient is known (25).

Finally, this theory can provide information on domain sizes. We have tested the theory by comparing fluorescence quenching curves obtained with small chlorophyll-protein complexes, aggreggates of such complexes, and whole chloroplast membranes. These results, as well as detailed considerations of the different types of competitive quenching (*i–iii*) will be treated in detail elsewhere.

COMPARISON WITH MAUZERALL'S STATISTICAL THEORY

Mauzerall (10, 14) has utilized a fundamentally different approach to calculate photochemical yields and fluorescence parameters of photosynthetic units subjected to multiple photon hits. As in our treatment, and, in fact, every other treatment in which the statistics of photon hits must be taken into account, Poisson distributions are utilized. Mauzerall has postulated several models to describe the effects of succeeding photon hits in a domain, including semi-annihilation and total annihilation of excitons, escape at closed and open traps, etc. (10); the kinetics of the system were treated by considering the basic decay parameters of the excitons in relation to the mean frequencies of excitation.

Our basic approach, while statistical in nature, is quite different and is based on solutions of the master equation in which the exciton and quencher (trap) parameters are specifically considered. Thus, our basic results are also quite different from those of Mauzerall's. The yields (photochemical as well as fluorescence), as embodied in Eq. 31, 32, and 44 are, in general, described by a series of weighted exponentials. The arguments of each exponential are a function of the quantum yields χ_i of transformation of quenchers ($Q_o \rightarrow Q_q$) and the number of photons absorbed in a domain; thus the history of the domains (in terms of the previous absorption of photons) is treated in a totally different way than in Mauzerall's case. Furthermore, the relative weights of each exponential in the series (Eqs. 31 and 32) depend on the size of the system (the parameter m) and R, the parameter that describes the fluorescence of the system in the limits of low and high excitation intensities.

It is shown here that our expression for the fluorescence and photochemical yields reduces to Mauzerall's "cumulative one-hit Poisson distribution" only under special circumstances: (*a*) when either $m = 1$ (the puddle model) for all values of R, or (*b*) $R = 1$ (no change in fluorescence yield as a function of intensity), and for all values of m (independent of the size of the photosynthetic unit). In all other cases the results of the two treatments are different.

APPENDIX

Solution of the Master Equation

To solve the Master Equation (Eq. 1), it is useful to introduce the quantities $M_{i,l}(t)$ defined as follows:

$$M_{i,l}(t) = \sum_{n=l}^{\infty} C_n^l \, p(i, n; t) \quad \text{where } C_n^l = \frac{n!}{(n-l)!l!}.$$

We can thus obtain (cf. Eqs. 15)

$$M_{i,0}(t) = \sum_{n=0}^{\infty} p(i, n; t) = p_i(t)$$

$$M_{i,1}(t) = \sum_{n=1}^{\infty} np(i, n; t) = n_i(t)$$

$$M_{i,2}(t) = \sum_{n=2}^{\infty} \frac{n(n-1)}{2} p(i, n; t) \text{ etc. . .} \qquad \text{(A1)}$$

Using Eq. 11 we obtain

$$\frac{dM_{i,l}}{dt} = -lK_i M_{i,l} + \sigma I M_{i_{i,l-1}}$$

$$-(l+1)K_i' M_{i,l+1} + (l+1)K_{i-1}', M_{i-1,l+1}. \qquad \text{(A2)}$$

This system of equations can be solved by supposing that starting with the rank $l \geq l_o$, $M_{il} \ll 1$. This is realized if $n_i(t) < l_o$. If the excitation intensity is sufficiently weak that $\sigma I \ll K_o, K_m$. One can choose $l_o = 2$.

The set of equations in A1, then, contains only two equations

$$\frac{dp_i}{dt} = -K_i' n_i + K_{i-1}' n_{i-1}$$

$$\frac{dn_i}{dt} = \sigma I p_i - K_i n_i \qquad \text{(A3)}$$

from which, if it is assumed that

$$\frac{dI}{Idt} \ll K_o, K_m,$$

one obtains

$$n_i \cong \frac{\sigma I p_i}{K_i}$$

and

$$\frac{dp_i}{\sigma I dt} = -\chi_i p_i + \chi_{i-1} p_{i-1} \qquad \text{(A4)}$$

where $\chi_i = (K_i'/K_i)$ (see Eq. 9). Eq. A4 can be rewritten as follows (see Eq. 19):

$$\frac{dp_i}{dY_t} = -\chi_i p_i + \chi_{i-1} p_{i-1}. \quad \text{(A5)}$$

We introduce the Laplace transformation $\tilde{p}_i(s)$

$$\tilde{p}_i(s) = \int_0^\infty e^{-sY_t} p_i(Y_t)\, dY_t$$

and the generating function $\tilde{Z}(z,s) = \Sigma_i\, \phi_i'\, \tilde{p}_i(s) z^i$ where (Eq. 27) $\phi_i' = (\phi_i - \phi_m)/(\phi_o - \phi_m)$. By using (A5) one obtains

$$z(z+a)\frac{\partial \tilde{Z}}{\partial z} = -b(z+a)\tilde{Z} + (m-1+b)z\tilde{Z} + \sum_{i=o}^{m} \frac{(m-i) z^i p_i(o)}{\chi_o} \quad \text{(A6)}$$

where $p_i(o)$ is the probability that there are i quenchers in the state Q_q at the time $t = o$, and

$$a = \frac{s}{\chi_o}\frac{1-R}{R} - 1$$

$$b = \frac{1}{a}(1 + s/\chi_o)m.$$

Eq. A6. can be easily integrated to give

$$\tilde{Z}(z,s) = \sum_{i=o}^{m} p_i(o)\frac{m-i}{\chi_o}\frac{1}{a^{m-i}} \cdot \sum_{j=i}^{m-1} C_{m-1-i}^{j-i}(-1)^{j-i}\left(\frac{z^j(z+a)^{m-1-j}}{b+j}\right). \quad \text{(A7)}$$

By setting $z = 1$ and by taking the inverse Laplace transformation, one obtains

$$\phi'(Y_t) = \sum_{i=0}^{m-1} p_i(0) \sum_{j=i}^{m-1} C_{m-1}^{j-i} \frac{R(1-R)^{m-1-j}}{m^{m-i-1}} (m-j)^{m-j}[j + (m-j)R]^{j-i-1} e^{-\chi_j Y_t} \quad \text{(A8)}$$

and from Eq. 29

$$\Phi'(Y) = \frac{1}{\chi_o Y}\sum_{i=o}^{m-1} p_i(o)\left[(m-i) - \sum_{j=i}^{m-1} C_{m-1}^{j-i}\frac{(1-R)^{m-1-j}}{m^{m-i-1}} (m-j)^{m-j-1}[j + (m-j)R]^{j-i} e^{-\chi_j Y}\right]. \quad \text{(A9)}$$

Furthermore, by expanding A.7 in powers of s one can calculate the different moments of $\phi'(Y_t)$:

$$\int_0^\infty \phi'(Y_t) dY_t = \sum_i p_i(o)\frac{m-i}{\chi_o}$$

$$\int_0^\infty Y_t \phi'(Y_t) dY_t = \frac{(m+i-1) + R(m-i)}{2\chi_o^2 R} \text{ etc. . .}$$

The Random Spatial Exciton Distribution Approximation

It is well established (see reference 27 for example) that this approximation is valid when the rate of transfer (Föster transfer rate per chlorophyll molecule multiplied by the number of nearest neighbor molecules) is rapid in comparison with the rate of capture K_i, (Eq. 6) of an exciton by a quencher molecule. Under these conditions, which may not hold for all photosynthetic organisms (28), the rate constant K_i is a linear function of the parameter $q = \langle i/m \rangle$ as implied in Eq. 6 (29). However, Paillotin has shown that this linear dependence of K_i on q may also be valid even when the spatial exciton distribution is not totally randomized (30). A detailed treatment of exciton motion (by the random hopping mechanism) in the presence of partially open and closed reaction centers gives the following expression for the relative instantaneous fluorescence yield as a function of q (30):

$$\frac{\phi}{\phi_m} = \frac{1}{1 + \dfrac{(1-q)(R-1)}{1 - K\ln(1-q)}} \quad \text{(A10)}$$

where

$$K = \left(\frac{k_F}{\phi_m}\right)\left(\frac{N(R-1)}{\pi L}\right) \quad \text{(A11)}$$

where N is the number of chlorophyll molecules per domain, and the parameters ϕ_m and R are defined in the text (Eq. 28).

When the condition

$$K|\ln(1-q)| \ll 1 \quad \text{(A12)}$$

is valid, Eq. 10 reduces to

$$\frac{\phi}{\phi_m} = \frac{1}{R + (1-R)q}$$

which is the Stern-Volmer relationship (Eq. 48) derived in the text. This equation is obtained when K_i is a linear function of q and thus justifies the use of Eq. 6.

To determine the conditions under which Inequality A12 is valid, we evaluate the quantity K in Eq. A11. We note that $\phi_m/k_F = \tau_m$, the exciton lifetime when all of the reaction centers are closed ($i = m$); in green plants $\tau_m = 2 \times 10^{-9}$ s (31). The transfer rate has been estimated to be $5 \times 10^{12} s^{-1}$ (32) and, using $N = 1{,}000$ (9), with a typical value of $R = 4$ (1, 12, 13), we obtain

$$|\ln(1-q)| \ll 10. \quad \text{(A13)}$$

Thus, the approximate form of Eq. A10 given by Eq. 48 is valid for most values of q, except when $q \to 1.0$ (almost all reaction centers closed).

We wish to thank Dr. C. E. Swenberg for several stimulating discussions.

This work was in part supported by a National Science Foundation grant PCM-8006109 to Dr. Geacintov at New York University. Partial support from a Department of Energy Contract No. E(II-I)2386 at the Radiation and Solid State Laboratory at New York University is also acknowledged.

Received for publication 31 August 1982 and in revised form 10 May 1983

REFERENCES

1. Lavorel, J., and A. L. Etienne. 1977. *In vivo* chlorophyll fluorescence. *Top. Photosyn.* 2:203–368.
2. Sonneveld, A., H. Rademaker, and L. N. M. Duysens. 1980. Transfer and trapping of excitation energy in photosystem II as studied by chlorophyll *a2* fluorescence quenching by dinitrobenzene and carotenoid triplet. The matrix model. *Biochim. Biophys. Acta.* 593:272–289.

3. Monger, R. G., and W. W. Parson. 1977. Singlet-triplet fusion in *rhodopseudomonas sphaeroides* chromatophores. A probe of the organization of the photosynthetic apparatus. *Biochim. Biophys. Acta.* 460:393–407.
4. Mathis, P., W. L. Butler and K. Satoh. 1979. Carotenoid triplet state and chlorophyll fluorescence quenching in chloroplasts and subchloroplast particles. *Photochem. Photobiol* 30:603–614.
5. Maroti, P., and J. Lavorel. 1979. Intensity and time-dependence of the carotenoid triplet quenching under light flashes of rectangular shape in chlorella. *Photochem. Photobiol.* 29:1147–1151.
6. Joliot, A., and P. Joliot. 1964. Etudes cinétiques de la réaction photochimique libérant l'oxygène au cours de la photosynthèse. *C.R. Acad. Sci. Paris.* 258:4622–4625.
7. Paillotin, G. 1976. Movement of excitations in the photosynthetic domains of photosystem II. *J. Theor. Biol.* 58:237–252.
8. Breton, J., N. E. Geacintov, and C. E. Swenberg. 1979. Quenching of fluorescence by triplet excited states in chloroplasts. *Biochim. Biophys. Acta.* 548:616–635.
9. Paillotin, G., C. E. Swenberg, J. Breton, and N. E. Geacintov. Analysis of picosecond laser-induced fluorescence phenomena in photosynthetic membranes utilizing a master equation approach. *Biophys. J.* 25:513–533.
10. Mauzerall, D. 1982. Statistical theory of the effect of multiple excitation in photosynthetic systems. *In* Biological Events Probed by Ultrafast Laser Spectroscopy. R. R. Alfano, editor, Academic Press, Inc., New York. 215–235.
11. Borisov, A. Yu, and V. I. Godik. 1973. Excitation energy transfer in photosynthesis. *Biochem. Biophys. Acta.* 301:227–248.
12. Murata, N., M. Nishimura, and A. Takamiya. 1966. Fluorescence of chlorophyll in photosynthetic systems. II. Induction of fluorescence in isolated spinach chloroplasts. *Biochim. Biophys. Acta.* 120:23–33.
13. Malkin, S., and B. Kok. 1966. Fluorescence induction studies in isolated chloroplasts. I. Number of components involved in the reaction and quantum yields. *Biochim. Biophys. Acta.* 126:413–432.
14. Mauzerall, D. 1976. Fluorescence and multiple excitation in photosynthetic systems. *J. Phys. Chem.* 80:2306–2309.
15. van Gorkom, H. J., M. P. J. Pulles, and A. L. Etienne. 1978. Fluorescence and absorption changes in Tris-washed chloroplasts. *In* Photosynthetic Oxygen Evolution. H. Metzner, editor. Academic Press, Inc. Ltd., London. 135–145.
16. Clayton, R. K. 1967. An analysis of the relations between fluorescence and photochemistry during photosynthesis. *J. Theor. Biol.* 14:173–186.
17. Wang, R. T., and M. Myers. 1973. Energy transfer between photosynthetic units analyzed by flash oxygen yield vs. flash intensity. *Photochem. Photobiol.* 17:321–332.
18. Jursinic, P. 1979. Flash-yield pattern for photosynthetic oxygen evolution in *Chlorella* and chloroplasts as a function of excitation intensity. *Arch. Biochem. Biophys.* 196:484–492.
19. Ley, A. C., and D. C. Mauzerall. 1982. Absolute absorption crossections for photosystem II and the minimum quantum requirement for photosynthesis in *Chlorella vulgaris. Biochim. Biophys. Acta.* 680:95–106.
20. Malkin, S. 1974. Energy transfer in the photosynthetic unit. I. The concept of independent units for photosystem II analyzed by flash yields for dichlorophenolindophenol reduction. *Biophys. Chem.* 2:327–337.
21. Joliot, P., P. Bennoun, and A. Joliot. 1973. New evidence supporting energy transfer between photosynthetic units. *Biochim. Biophys. Acta.* 305:317–328.
22. Horton, P. 1981. The effect of redox potential on the kinetics of fluorescence induction in pea chloroplasts. II. Sigmoidicity. *Biochim. Biophys. Acta.* 637:152–158.
23. Joliot, P., and A. Joliot. 1973. Different types of quenching involved in photosystem II centers. *Biochim. Biophys. Acta.* 305:302–316.
24. Geacintov, N. E., and J. Breton. 1982. Laser studies of primary processes in photosynthesis. *In* Trends in Photobiology. C. Helene, M. Charlier, Th. Montenay-Garestier and G. Laustriat, editors. Plenum Publishing Corp., New York. 549–559.
25. Geacintov, N. E., J. Breton, C. E. Swenberg, and G. Paillotin. 1977. A single pulse picosecond laser study of exciton dynamics in chloroplasts. *Photochem. Photobiol.* 26:629–638; 29:651–652.
26. Swenberg, C. E., N. E. Geacintov, and M. Pope. 1976. Bimolecular quenching of excitons and fluorescence in the photosynthetic unit. *Biophys. J.* 16:1447–1452.
27. Huber, D. L. 1979. Fluorescence in the presence of traps. *Phys. Rev. B.* 20:2307–2314.
28. Pearlstein, R. M. 1982. Exciton migration and trapping in photosynthesis. *Photochem. Photobiol.* 35:835–844.
29. Fay, D. 1982. Configuration average for energy transfer to randomly distributed acceptors in the fast-migration limit. *Phys. Rev. B.* 25:4245–4247.
30. G. Paillotin. 1974. Etude theorique des modes de creation, de transport et d'utilisation de l'energie d'excitation electronique chez les plantes superieures. Ph. D. Dissertation, Université Paris-Sud (Orsay).
31. Breton, J., and N. E. Geacintov. 1980. Picosecond fluorescence kinetics and fast energy transfer processes in photosynthetic membranes. *Biochim. Biophys. Acta.* 594:1–32.
32. Paillotin, G. 1976. Capture frequency of excitations and energy transfer between photosynthetic units in photosystem II. *J. Theor. Biol.* 58:219–235.